Probing New Physics through B Mixing:
Status, Benchmarks and Prospects

Patricia Ball[a,b] **and Robert Fleischer**[b]

[a] *IPPP, Department of Physics, University of Durham, Durham DH1 3LE, UK*

[b] *Theory Division, Department of Physics, CERN, CH-1211 Geneva 23, Switzerland*

Abstract

As is well known, $B_{d,s}^0$–$\bar{B}_{d,s}^0$ mixing offers a profound probe into the effects of physics beyond the Standard Model. The data obtained at the e^+e^- B factories have already provided valuable insights into the B_d-meson system, and very recently also the B_s^0–$\bar{B}_s^0$ oscillation frequency ΔM_s has been measured at the Tevatron. We give a critical discussion of the interpretation of these data in terms of model-independent new-physics parameters. We address in particular the impact of the uncertainties of the relevant input parameters, set benchmarks for their accuracies as required by future precision measurements at the LHC, and explore the prospects for new CP-violating effects in the B_s system. To complement our model-independent analysis, we also discuss the constraints imposed by the CDF measurement of ΔM_s on popular models of new physics, namely scenarios with an extra Z' boson and supersymmetry. We find that the new data still leave sizeable room for new-physics contributions to B_s^0–$\bar{B}_s^0$ mixing, which could be detected at the LHC.

April 2006

1 Introduction

One of the most promising ways to detect the effects of new physics (NP) on B decays is to look for deviations of flavour-changing neutral-current (FCNC) processes from their Standard Model (SM) predictions; FCNC processes only occur at the loop-level in the SM and hence are particularly sensitive to NP virtual particles and interactions. A prominent example that has received extensive experimental and theoretical attention is B_q^0–$\bar{B}_q^0$ mixing ($q \in \{d, s\}$), which, in the SM, is due to box diagrams with W-boson and up-type quark exchange. In the language of effective field theory, these diagrams induce an effective Hamiltonian, which causes B_q^0 and $\bar{B}_q^0$ mesons to mix and generates a $\Delta B = 2$ transition:

$$\langle B_q^0 | \mathcal{H}_{\text{eff}}^{\Delta B=2} | \bar{B}_q^0 \rangle = 2 M_{B_q} M_{12}^q \,, \tag{1}$$

where M_{B_q} is the B_q-meson mass. Thanks to B_q^0–$\bar{B}_q^0$ mixing, an initially present B_q^0 state evolves into a time-dependent linear combination of B_q^0 and $\bar{B}_q^0$ flavour states. The oscillation frequency of this phenomenon is characterized by the mass difference of the "heavy" and "light" mass eigenstates,

$$\Delta M_q \equiv M_{\text{H}}^q - M_{\text{L}}^q = 2 |M_{12}^q| \,, \tag{2}$$

and the CP-violating mixing phase

$$\phi_q = \arg M_{12}^q \,, \tag{3}$$

which enters "mixing-induced" CP violation. The mass difference ΔM_q can be – and has been – measured from the proper-time distribution of B_q^0 candidates identified through their decays into (mostly) flavour-specific modes, after having been tagged as mixed or unmixed. The current experimental results are

$$\Delta M_d = (0.507 \pm 0.004)\,\text{ps}^{-1} \,, \qquad \Delta M_s = \left[17.33^{+0.42}_{-0.21}(\text{stat}) \pm 0.07(\text{syst}) \right] \text{ps}^{-1} \,, \tag{4}$$

where the value of ΔM_d is the world average quoted by the "Heavy Flavour Averaging Group" (HFAG) [1]. Concerning ΔM_s, only lower bounds were available for many years from the LEP experiments at CERN and SLD at SLAC [2]. Since the currently operating $e^+ e^-$ B factories run at the $\Upsilon(4S)$ resonance, which decays into $B_{u,d}$, but not into B_s mesons, the B_s system cannot be explored by the BaBar and Belle experiments. However, plenty of B_s mesons are produced at the Tevatron (and later on will be at the LHC), which – very recently – allowed the CDF collaboration to measure ΔM_s with the result given above [3]; the D0 collaboration has provided, also very recently, a two-sided bound on ΔM_s at the 90% C.L. [4]:

$$17\,\text{ps}^{-1} < \Delta M_s < 21\,\text{ps}^{-1}, \tag{5}$$

which is compatible with the CDF measurement and corresponds to a $2.5\,\sigma$ signal at $\Delta M_s = 19\,\text{ps}^{-1}$. These new results from the Tevatron have already triggered a couple of phenomenological papers [5]–[11].

In the SM, M_{12}^q is given by

$$M_{12}^{q,\text{SM}} = \frac{G_{\text{F}}^2 M_W^2}{12\pi^2} M_{B_q} \hat{\eta}^B \hat{B}_{B_q} f_{B_q}^2 (V_{tq}^* V_{tb})^2 S_0(x_t) \,, \tag{6}$$

where G_F is Fermi's constant, M_W the mass of the W boson, $\hat{\eta}^B = 0.552$ a short-distance QCD correction (which is the same for the B_d^0 and B_s^0 systems) [12], whereas the "bag" parameter $\hat{B}_{B_q}$ and the decay constant f_{B_q} are non-perturbative quantities. V_{tq} and V_{tb} are elements of the Cabibbo–Kobayashi–Maskawa (CKM) matrix [13, 14], and $S_0(x_t \equiv \overline{m}_t^2/M_W^2) = 2.35 \pm 0.06$ with $\overline{m}_t(m_t) = (164.7 \pm 2.8)\,\text{GeV}$ [15] is one of the "Inami–Lim" functions [16], describing the t-quark mass dependence of the box diagram with internal t-quark exchange; the contributions of internal c and u quarks are, by virtue of the Glashow–Iliopoulos–Maiani (GIM) mechanism [17], suppressed by $(m_{u,c}/M_W)^2$.

The mixing phases ϕ_q can be measured from "mixing-induced" CP asymmetries. In the SM, one has

$$\phi_d^{\text{SM}} = 2\beta, \qquad \phi_s^{\text{SM}} = -2\delta\gamma, \tag{7}$$

where β is the usual angle of the "conventional" unitarity triangle (UT) of the CKM matrix, while $\delta\gamma$ characterizes another unitarity triangle [18] that differs from the UT through $\mathcal{O}(\lambda^2)$ corrections in the Wolfenstein expansion [19].[1]

The purpose of this paper is to explore the possibility that B_q^0–$\bar{B}_q^0$ mixing is modified by NP contributions at the tree level and/or new particles in the loops. We shall find in particular that – despite the apparently strong constraints posed by the precise measurements of ΔM_q in Eq. (4) – these results can contain potentially large NP contributions, which presently cannot be detected.

The outline of our paper is as follows: in Section 2, we collect the input parameters of our analysis and discuss the status of the relevant hadronic uncertainties. In Sections 3 and 4, we then focus on the B_d- and B_s-meson systems, respectively, and investigate, in a model-independent way, the size of possible NP contributions to ΔM_q and ϕ_q in the light of present and future experimental measurements and hadronic uncertainties. In this analysis, we consider also a scenario for the experimental and theoretical situation in the year 2010, and set benchmarks for the required accuracy of the relevant hadronic parameters. It turns out that the situation in the B_s system is more favourable than in the B_d system, and that still ample space for NP effects in B_s^0–$\bar{B}_s^0$ mixing is left, which could be detected at the LHC. In Section 5, we complement the model-independent discussion of Sections 3 and 4 by analyses of two specific scenarios for NP: models with an extra Z' boson and supersymmetry (SUSY) with an approximate alignment of quark and squark masses. We summarize our conclusions in Section 6.

2 Input Parameters and Hadronic Uncertainties

2.1 CKM Parameters

Before going into the details of B_q^0–$\bar{B}_q^0$ mixing and possible NP effects, let us first have a closer look at the relevant input parameters and their uncertainties. Throughout our analysis, we assume that the CKM matrix is unitary, and shall use this feature to express the CKM elements entering B_q^0–$\bar{B}_q^0$ mixing in terms of quantities that can be determined

---

[1]Throughout this paper, we use the phase convention for the CKM matrix advocated by the Particle Data Group [20], where the decay amplitudes of $b \to c\bar{c}s$ processes carry essentially no CP-violating weak phase. Physical CP asymmetries are of course independent of the applied CKM phase convention, as shown explicitly in Ref. [21].

through tree-level processes of the SM. The key rôle is then played by $|V_{cb}|$ and $|V_{ub}|$. The former quantity is presently known with 2% precision from semileptonic B decays; in this paper we shall use the value obtained in Ref. [22] from the analysis of leptonic and hadronic moments in inclusive $b \to c\ell\bar{\nu}_\ell$ transitions [23]:

$$|V_{cb}| = (42.0 \pm 0.7) \cdot 10^{-3} \, ; \tag{8}$$

this value agrees with that from exclusive decays.

The situation is less favourable with $|V_{ub}|$: there is a 1σ discrepancy between the values from inclusive and exclusive $b \to u\ell\bar{\nu}_\ell$ transitions [1]:

$$|V_{ub}|_{\text{incl}} = (4.4 \pm 0.3) \cdot 10^{-3} \, , \qquad |V_{ub}|_{\text{excl}} = (3.8 \pm 0.6) \cdot 10^{-3} \, . \tag{9}$$

The error on $|V_{ub}|_{\text{excl}}$ is dominated by the theoretical uncertainty of lattice and light-cone sum rule calculations of $B \to \pi$ and $B \to \rho$ transition form factors [24, 25], whereas for $|V_{ub}|_{\text{incl}}$ experimental and theoretical errors are at par. We will use both results in our analysis.

Whereas any improvement of the error of $|V_{cb}|$ will have only marginal impact on the analysis of B mixing, a reduction of the uncertainty of $|V_{ub}|$ will be very relevant. As a benchmark scenario for the situation in 2010, we will assume that the central value of $|V_{ub}|_{\text{incl}}$ gets confirmed and that its uncertainty will shrink to $\pm 0.2 \cdot 10^{-3}$, i.e. 5%, thanks to better statistics and an increased precision of theoretical predictions, for instance from further developments in the dressed gluon exponentiation [26].

2.2   Hadronic Mixing Parameters $f_{B_q} \hat{B}_{B_q}^{1/2}$

The next ingredient in the SM prediction for $M_{12}^{q,\text{SM}}$ are the non-perturbative matrix elements $f_{B_q}^2 \hat{B}_{B_q}$. These parameters have been the subject of numerous lattice calculations, both quenched and unquenched, using various lattice actions and implementations of both heavy and light quarks. The current front runners are unquenched calculations with 2 and 3 dynamical quarks, respectively, and Wilson or staggered light quarks. Despite tremendous progress in recent years, the results still suffer from a variety of uncertainties which is important to keep in mind when interpreting and using lattice results. One particular difficulty in determining f_{B_d} is the chiral extrapolation needed to go to the physical d-quark mass.[2] Lattice calculations are usually performed at unphysically large u- and d-quark masses, as the simulation of dynamical fermions involves many inversions of the fermions' functional determinant in the path integral and is very dear in terms of CPU time. Therefore, an extrapolation, called the chiral extrapolation, in the light-quark masses from feasible to physical masses is necessary, which is done using the functional form predicted by chiral perturbation theory. Based on these arguments, the chiral extrapolation of $\hat{B}_{B_d}$ to the physical limit is expected to be smooth, whereas that of f_{B_d} is potentially prone to logarithms [28], which leads to a considerable increase in the uncertainty. The most recent (unquenched) simulation by the JLQCD collaboration [29],

---

[2]Many lattice simulations do not distinguish between u- and d-quark masses and use $m_{u,d} \equiv (m_u + m_d)/2$. The physical value of the light-quark mass ratio is then $m_{u,d}/m_s = 0.041 \pm 0.003$ from chiral perturbation theory [27].

with non-relativistic b quarks and two flavours of dynamical light (Wilson) quarks, yields $f_{B_d} = (0.191 \pm 0.010^{+0.012}_{-0.022})\,\mathrm{GeV}$ and

$$f_{B_d}\hat{B}^{1/2}_{B_d}\Big|_{\mathrm{JLQCD}} = (0.215 \pm 0.019^{+0}_{-0.023})\,\mathrm{GeV}\,,$$

$$f_{B_s}\hat{B}^{1/2}_{B_s}\Big|_{\mathrm{JLQCD}} = (0.245 \pm 0.021^{+0.003}_{-0.002})\,\mathrm{GeV}\,,$$

$$\xi_{\mathrm{JLQCD}} \equiv \frac{f_{B_s}\hat{B}^{1/2}_{B_s}}{f_{B_d}\hat{B}^{1/2}_{B_d}}\Bigg|_{\mathrm{JLQCD}} = 1.14 \pm 0.06^{+0.13}_{-0}\,, \tag{10}$$

where the first error includes uncertainties from statistics and various systematics, whereas the second, asymmetric error comes from the chiral extrapolation. Note that part of the systematic errors cancel in the ratio ξ. In this calculation, the ratio $m_{u,d}/m_s$ was varied between 0.7 and 2.9.

More recently, (unquenched) simulations with three dynamical flavours have become possible using staggered quark actions. The HPQCD collaboration obtains $f_{B_d} = (0.216 \pm 0.022)\,\mathrm{MeV}$ [30], where a ratio of $m_{u,d}/m_s$ as small as 0.125 could be achieved, due to the good chiral properties of the staggered action. This implies that the chiral extrapolation is less critical and the corresponding error much smaller. The quoted error on f_{B_q} is now dominated by yet uncalculated higher-order matching terms which are needed to match the (effective theory) lattice calculations to continuum QCD. Lacking any direct calculation of $\hat{B}_{B_q}$ with three dynamical flavours, and in view of the fact that the bag parameter is likely to be less sensitive to chiral extrapolation, it has been suggested to combine the results of f_{B_q} from HPQCD with that of $\hat{B}_{B_q}$ from JLQCD, yielding [31]:

$$f_{B_d}\hat{B}^{1/2}_{B_d}\Big|_{\mathrm{(HP+JL)QCD}} = (0.244 \pm 0.026)\,\mathrm{GeV}\,,$$

$$f_{B_s}\hat{B}^{1/2}_{B_s}\Big|_{\mathrm{(HP+JL)QCD}} = (0.295 \pm 0.036)\,\mathrm{GeV}\,,$$

$$\xi_{\mathrm{(HP+JL)QCD}} = 1.210^{+0.047}_{-0.035}\,, \tag{11}$$

where all errors are added in quadrature.

Although we shall use both (10) and (11) in our analysis, we would like to stress that the errors are likely to be optimistic. Apart from the issue of the chiral extrapolation discussed above, there is also the question of discretisation effects (JLQCD uses data obtained at only one lattice spacing) and the renormalisation of matrix elements (for lattice actions without chiral symmetry, the axial vector current is not conserved and f_{B_q} needs to be renormalised), which some argue should be done in a non-perturbative way [32]. Simulations with staggered quarks also face potential problems with unitarity, locality and an odd number of flavours (see, for instance, Ref. [33]). A confirmation of the HPQCD results by simulations using the (theoretically better understood) Wilson action with small quark masses will certainly be highly welcome.

Given this situation, we consider it not very likely that the errors on f_{B_q}, $\hat{B}_{B_q}$ and ξ will come down considerably in the near future. For our benchmark 2010 scenario, we hence will assume the values of hadronic parameters and uncertainties given in (11).

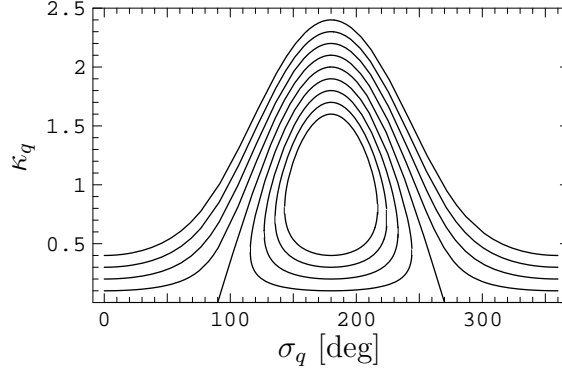We are now well prepared for the discussion of B^0_q–$\bar{B}^0_q$ mixing.

Figure 1: The dependence of κ_q on σ_q for values of ρ_q varied between 1.4 (most upper curve) and 0.6 (most inner curve), in steps of 0.1. The contours apply to both the $q = d$ and the $q = s$ system.

3   The B_d-Meson System

3.1   Model-Independent NP Parameters

Let us first have a closer look at the B_d^0–$\bar{B}_d^0$ mixing parameters. In the presence of NP, the matrix element M_{12}^d can be written, in a model-independent way, as

$$M_{12}^d = M_{12}^{d,\text{SM}} \left(1 + \kappa_d e^{i\sigma_d}\right) ,$$

where the real parameter $\kappa_d \geq 0$ measures the "strength" of the NP contribution with respect to the SM, whereas σ_d is a new CP-violating phase; analogous formulae apply to the B_s system. The B_d mixing parameters then read

$$\Delta M_d = \Delta M_d^{\text{SM}} \left[1 + \kappa_d e^{i\sigma_d}\right], \tag{12}$$

$$\phi_d = \phi_d^{\text{SM}} + \phi_d^{\text{NP}} = \phi_d^{\text{SM}} + \arg(1 + \kappa_d e^{i\sigma_d}) . \tag{13}$$

The experimental result for ΔM_d and the theoretical prediction ΔM_d^{SM} provide the following constraint on κ_d and σ_d:

$$\rho_d \equiv \left| \frac{\Delta M_d}{\Delta M_d^{\text{SM}}} \right| = \sqrt{1 + 2\kappa_d \cos \sigma_d + \kappa_d^2}, \tag{14}$$

which determines, for instance, κ_d as function of σ_d:

$$\kappa_d = -\cos \sigma_d \pm \sqrt{\rho_d^2 - \sin^2 \sigma_d} . \tag{15}$$

In Fig. 1, we illustrate the corresponding contours in the σ_d–κ_d plane for values of ρ_d between 0.6 and 1.4, varied in steps of 0.1. Interestingly enough, a value of ρ_d smaller than 1 imposes a constraint on the weak NP phase σ_d:

$$\pi - \arcsin \rho_d \leq \sigma_d \leq \pi + \arcsin \rho_d. \tag{16}$$

3.2 The SM Prediction for ΔM_d

In order to make use of these constraints, one needs to know the SM prediction ΔM_d^{SM}. In particular, one has to make sure that the parameters entering $M_{12}^{d,\mathrm{SM}}$, Eq. (6), are free from NP. This can be achieved, to very good accuracy, by expressing the relevant CKM factor in ΔM_d^{SM} in terms of parameters measured in tree-level processes. To this end, we use the Wolfenstein parametrization [19], as generalized in Ref. [34], and the unitarity of the CKM matrix to write

$$|V_{td}^* V_{tb}| = |V_{cb}|\lambda\sqrt{1 - 2R_b\cos\gamma + R_b^2}\,. \tag{17}$$

Here the quantity R_b is given by

$$R_b \equiv \left(1 - \frac{\lambda^2}{2}\right)\frac{1}{\lambda}\left|\frac{V_{ub}}{V_{cb}}\right| = \sqrt{\bar{\rho}^2 + \bar{\eta}^2}, \tag{18}$$

with

$$\bar{\rho} = (1 - \lambda^2/2)\rho = R_b\cos\gamma, \quad \bar{\eta} = (1 - \lambda^2/2)\eta = R_b\sin\gamma\,; \tag{19}$$

R_b measures one side of the UT, and γ denotes the usual UT angle.

As we saw in Section 2, $|V_{cb}|$ and $|V_{ub}|$ can be determined from semileptonic B decays, which arise at tree level in the SM and hence are very robust with respect to NP effects. A similar comment applies to the Wolfenstein parameter $\lambda \equiv |V_{us}|$ [19, 34], which can be determined, for instance, from $K \to \pi\ell\bar{\nu}_\ell$ decays. Using the values of $|V_{cb}|$ and $|V_{ub}|$ discussed in Section 2 and $\lambda = 0.225 \pm 0.001$ [35], we obtain

$$R_b^{\mathrm{incl}} = 0.45 \pm 0.03\,, \qquad R_b^{\mathrm{excl}} = 0.39 \pm 0.06\,, \tag{20}$$

where the labels "incl" and "excl" refer to the determinations of $|V_{ub}|$ through inclusive and exclusive $b \to u\ell\bar{\nu}_\ell$ transitions, respectively.

The angle γ can be determined in a variety of ways through CP-violating effects in pure tree decays of type $B \to D^{(*)}K^{(*)}$ [36]. Using the present B-factory data, the following results were obtained through a combination of various methods:

$$\gamma|_{D^{(*)}K^{(*)}} = \begin{cases} (62^{+35}_{-25})^\circ & \text{(CKMfitter collaboration [37])}, \\ (65 \pm 20)^\circ & \text{(UTfit collaboration [38])}. \end{cases} \tag{21}$$

A more precise value for γ was obtained in Ref. [39], from the B-factory data on CP asymmetries in $B_d^0 \to \pi^+\pi^-$ and $B_d^0 \to \pi^- K^+$ decays, which receive both tree and penguin contributions:

$$\gamma|_{\pi^+\pi^-, \pi^- K^+} = (73.9^{+5.8}_{-6.5})^\circ. \tag{22}$$

Within the NP scenario of modified electroweak penguins considered in Ref. [39], (22) is not affected by NP effects. The central value of (22) is higher than that of (21), but both results are perfectly consistent because of the large errors of the $B \to D^{(*)}K^{(*)}$ determinations. An even larger value of γ in the ballpark of 80° was recently extracted from $B \to \pi\pi$ data with the help of "soft collinear effective theory" (SCET) [40].

In our analysis, we use the UTfit value
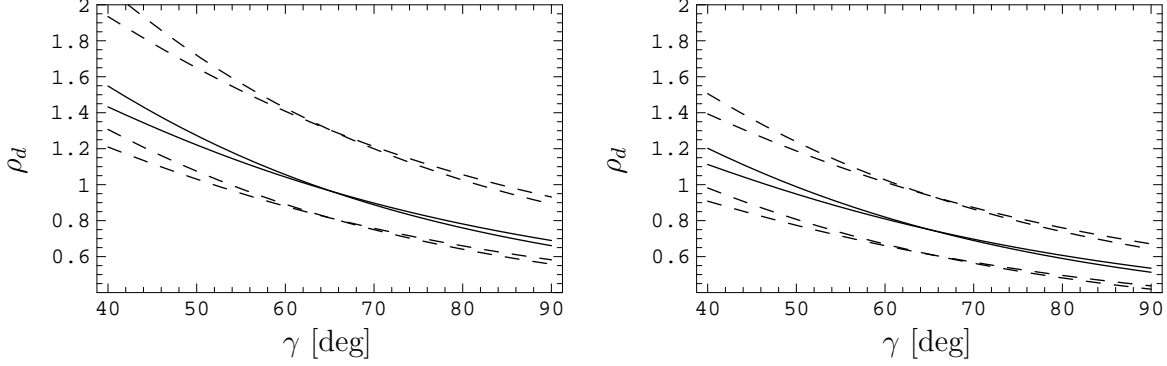
$$\gamma = (65 \pm 20)^\circ. \tag{23}$$

Figure 2: The dependence of ρ_d on γ for $R_b = (0.39, 0.45)$ and various values of $f_{B_d}\hat{B}_{B_d}^{1/2}$. Left panel: JLQCD results (10): $f_{B_d}\hat{B}_{B_d}^{1/2} = 0.215\,\mathrm{GeV}$ (solid lines), $f_{B_d}\hat{B}_{B_d}^{1/2} = (0.185, 0.234)\,\mathrm{GeV}$ (dashed lines). Right panel: ditto for (HP+JL)QCD results (11): $f_{B_d}\hat{B}_{B_d}^{1/2} = 0.244\,\mathrm{GeV}$ (solid lines), $f_{B_d}\hat{B}_{B_d}^{1/2} = (0.218, 0.270)\,\mathrm{GeV}$ (dashed lines).

With the help of (8), (17) and (20), we then obtain

$$|V_{td}^*V_{tb}|_{\mathrm{incl}} = (8.6 \pm 1.5) \cdot 10^{-3}\,, \qquad |V_{td}^*V_{tb}|_{\mathrm{excl}} = (8.6 \pm 1.3) \cdot 10^{-3}\,, \tag{24}$$

where the uncertainty is dominated by that of the angle γ.

For our 2010 benchmark scenario, we assume that the central value of γ will settle at $70°$, and that the error will shrink to $\pm 5°$ thanks to strategies using pure tree decays of $B_{u,d}$ and B_s mesons for the determination of γ, which can be implemented at the LHC. In fact, a statistical accuracy of $\sigma_{\mathrm{stat}}(\gamma) \approx 2.5°$ is expected at LHCb after 5 years of taking data [41].

For the convenience of the reader, we summarise all CKM input parameters, as well as their counterparts for the B_s system to be discussed in Section 4, in Tab. 1; in Tab. 2, we give the input data for our 2010 scenario.

In Fig. 2, we illustrate the dependence of ρ_d defined in (14) on γ, R_b and $f_{B_d}\hat{B}_{B_d}^{1/2}$. It is evident that ρ_d depends rather strongly on γ and $f_{B_d}\hat{B}_{B_d}^{1/2}$, but less so on R_b. For the two different lattice results, we obtain

$$\Delta M_d^{\mathrm{SM}}\Big|_{\mathrm{JLQCD}} = \left[0.52 \pm 0.17(\gamma, R_b)_{+0.13}^{-0.09}(f_{B_d}\hat{B}_{B_d}^{1/2})\right]\,\mathrm{ps}^{-1}\,,$$

$$\rho_d|_{\mathrm{JLQCD}} = 0.97 \pm 0.33(\gamma, R_b)_{+0.26}^{-0.17}(f_{B_d}\hat{B}_{B_d}^{1/2})\,,$$

$$\Delta M_d^{\mathrm{SM}}\Big|_{\mathrm{(HP+JL)QCD}} = \left[0.69 \pm 0.13(\gamma, R_b) \pm 0.08(f_{B_d}\hat{B}_{B_d}^{1/2})\right]\,\mathrm{ps}^{-1}\,,$$

$$\rho_d|_{\mathrm{(HP+JL)QCD}} = 0.75 \pm 0.25(\gamma, R_b) \pm 0.16(f_{B_d}\hat{B}_{B_d}^{1/2})\,, \tag{25}$$

where we made explicit the errors arising from the uncertainties of (γ, R_b) and $f_{B_d}\hat{B}_{B_d}^{1/2}$. These results are compatible with the SM value $\rho_d = 1$, but suffer from considerable uncertainties, which presently leave sizeable room for NP contributions to ΔM_d; we shall quantify below the allowed values of κ_d and σ_d following from the contours in Fig. 1.

Parameter	Value	Ref.	Remarks
λ	0.225 ± 0.001	[35]	CKM05 average
$|V_{cb}|$	$(42.0 \pm 0.7) \cdot 10^{-3}$	[22]	inclusive $b \to c\ell\bar{\nu}_\ell$
$|V_{ub}|_{\text{incl}}$	$(4.4 \pm 0.3) \cdot 10^{-3}$	[1]	our average
$|V_{ub}|_{\text{excl}}$	$(3.8 \pm 0.6) \cdot 10^{-3}$	[1]	our average
γ	$(65 \pm 20)^\circ$	[38]	UTfit average
R_b^{incl}	0.45 ± 0.03	Eq. (18)	
R_b^{excl}	0.39 ± 0.06	Eq. (18)	
R_t	0.91 ± 0.16	Eq. (39)	error dominated by γ
$|V_{td}^* V_{tb}|_{\text{incl}}$	$(8.6 \pm 1.5) \cdot 10^{-3}$	Eq. (17)	error dominated by γ
$|V_{td}^* V_{tb}|_{\text{excl}}$	$(8.6 \pm 1.3) \cdot 10^{-3}$	Eq. (17)	error dominated by γ
$|V_{ts}^* V_{tb}|$	$(41.3 \pm 0.7) \cdot 10^{-3}$	Eq. (35)	
β_{incl}	$(26.7 \pm 1.9)^\circ$	Eq. (32)	error dominated by R_b
β_{excl}	$(22.9 \pm 3.8)^\circ$	Eq. (32)	error dominated by R_b

Table 1: CKM parameters used in our analysis. All parameters are determined using input from tree-level processes only and the unitarity of the CKM matrix.

Parameter	Value
λ	0.225 ± 0.001
$|V_{cb}|$	$(42.0 \pm 0.7) \cdot 10^{-3}$
$|V_{ub}|$	$(4.4 \pm 0.2) \cdot 10^{-3}$
γ	$(70 \pm 5)^\circ$
R_b	0.45 ± 0.02
R_t	0.95 ± 0.04
$|V_{td}^* V_{tb}|$	$(8.9 \pm 0.4) \cdot 10^{-3}$
$|V_{ts}^* V_{tb}|$	$(41.3 \pm 0.7) \cdot 10^{-3}$
β	$(26.6 \pm 1.2)^\circ$
$f_{B_d} \hat{B}_{B_d}^{1/2}$	$(0.244 \pm 0.026)\,\text{GeV}$
$f_{B_s} \hat{B}_{B_s}^{1/2}$	$(0.295 \pm 0.036)\,\text{GeV}$
ρ_d	0.69 ± 0.16
ρ_s	0.74 ± 0.18
ξ	$1.210^{+0.047}_{-0.035}$
ρ_s/ρ_d	1.07 ± 0.12

Table 2: Benchmark values and uncertainties for CKM and hadronic parameters in 2010.
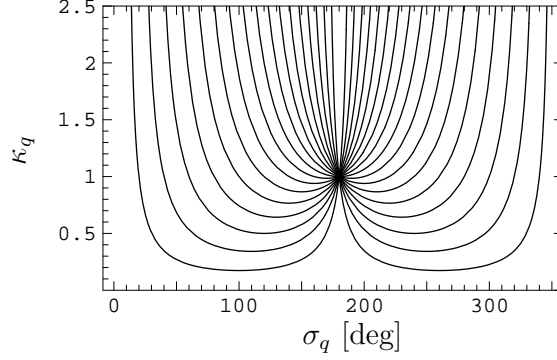
Figure 3: The dependence of κ_q on σ_q for values of ϕ_q^{NP} varied between $\pm 10°$ (lower curves) and $\pm 170°$ in steps of $10°$: the curves for $0° < \sigma_q < 180°$ and $180° < \sigma_q < 360°$ correspond to positive and negative values of ϕ_q^{NP}, respectively. The contours apply to both the $q = d$ and the $q = s$ system.
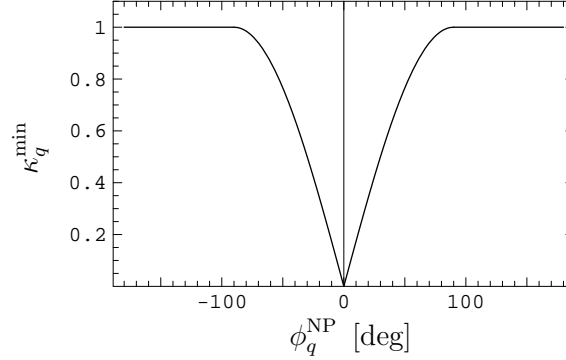

Figure 4: The minimum value κ_q^{min} of κ_q as function of the NP mixing phase ϕ_q^{NP}.

3.3   Constraints on NP through CP Violation: ϕ_d

The second constraint on the allowed values of κ_d and σ_d is provided by the experimental value of the B_d mixing phase $\phi_d = \phi_d^{\mathrm{SM}} + \phi_d^{\mathrm{NP}}$. Using (13), a given value of ϕ_d^{NP} allows one to determine κ_d as a function of σ_d with the help of the following expressions, which hold again in the general case $q \in \{d, s\}$:

$$\kappa_q = \frac{\tan \phi_q^{\mathrm{NP}}}{\sin \sigma_q - \cos \sigma_q \tan \phi_q^{\mathrm{NP}}}, \tag{26}$$

$$\sin \phi_q^{\mathrm{NP}} = \frac{\kappa_q \sin \sigma_q}{\sqrt{1 + 2\kappa_q \cos \sigma_q + \kappa_q^2}}, \quad \cos \phi_q^{\mathrm{NP}} = \frac{1 + \kappa_q \cos \sigma_q}{\sqrt{1 + 2\kappa_q \cos \sigma_q + \kappa_q^2}}. \tag{27}$$

In Fig. 3, we illustrate the corresponding contours for various values of ϕ_q^{NP}. Note in particular that κ_q is bounded from below for any given value of $\phi_q^{\mathrm{NP}} \neq 0$. The relation between the allowed values of ϕ_q^{NP} and κ_q is given by

$$\phi_q^{\mathrm{NP,max(min)}} = \arg\left\{1 + \kappa_q\left(-\kappa_q^2 \pm i\sqrt{1 - \kappa_q^2}\right)\right\}, \tag{28}$$

i.e. for any non-zero value of ϕ_q^{NP}, κ_q must be larger than the minimum value plotted in Fig. 4.

9

In order to make use of these theoretically clean contours, one needs to determine the NP phase ϕ_q^{NP}. As is well known, ϕ_d can be experimentally accessed in the mixing-induced CP asymmetry of the "golden" decay $B_d^0 \to J/\psi K_{\mathrm{S}}$ (and similar $b \to c\bar{c}s$ charmonium modes) [42]. The most recent average of the B-factory data for such transitions obtained by HFAG is [1]

$$(\sin\phi_d)_{c\bar{c}s} = 0.687 \pm 0.032 \,. \tag{29}$$

In principle, this quantity could be affected by NP contributions to both B_d^0–$\bar{B}_d^0$ mixing and $b \to c\bar{c}s$ decay amplitudes [43, 44]. A probe of the latter effects is provided by decays like $B_d \to D\pi^0, D\rho^0, \ldots$, which are pure tree decays and do not receive any penguin contributions. If the neutral D mesons are observed through their decays into CP eigenstates $D_\pm$, these decays allow an extremely clean determination of the "true" value of $\sin\phi_d$ [45]. A possible discrepancy with $(\sin\phi_d)_{c\bar{c}s}$ would be attributed to NP contributions to the $b \to c\bar{c}s$ decay amplitudes. Consequently, detailed feasibility studies for the exploration of $B_d \to D\pi^0, D\rho^0, \ldots$ modes at a super-B factory are strongly encouraged. In this paper, however, we assume that NP effects entering decay amplitudes are negligible. Eq. (13) then gives the following expression:

$$(\sin\phi_d)_{c\bar{c}s} \equiv \sin\phi_d = \sin(2\beta + \phi_d^{\mathrm{NP}})\,. \tag{30}$$

The experimental value (29) yields the twofold solution

$$\phi_d = (43.4 \pm 2.5)^\circ \quad \vee \quad (136.6 \pm 2.5)^\circ, \tag{31}$$

where the latter result is in dramatic conflict with global CKM fits and would require a large NP contribution to B_d^0–$\bar{B}_d^0$ mixing [46, 47]. However, experimental information on the sign of $\cos\phi_d$ rules out a negative value of this quantity at greater than 95% C.L. [36], so that we are left with $\phi_d = (43.4 \pm 2.5)^\circ$.

The SM prediction of the mixing phase, $\phi_d^{\mathrm{SM}} = 2\beta$, Eq. (7), can easily be obtained in terms of the tree-level quantities R_b and γ, as

$$\sin\beta = \frac{R_b \sin\gamma}{\sqrt{1 - 2R_b \cos\gamma + R_b^2}}\,, \quad \cos\beta = \frac{1 - R_b \cos\gamma}{\sqrt{1 - 2R_b \cos\gamma + R_b^2}}\,. \tag{32}$$

Using Eq. (13), the experimental value of ϕ_d can then immediately be converted into a result for the NP phase ϕ_d^{NP}, which depends on γ and R_b as illustrated in Fig. 5. It is evident that the dependence of ϕ_d^{NP} on γ is very small and that R_b plays actually the key rôle for its determination. Hence, we have a situation complementary to that shown in Fig. 2, where the main dependence was on γ. The parameters collected in Tab. 1 yield

$$\phi_d^{\mathrm{SM}}\Big|_{\mathrm{incl}} = (53.4 \pm 3.8)^\circ\,, \qquad \phi_d^{\mathrm{SM}}\Big|_{\mathrm{excl}} = (45.8 \pm 7.6)^\circ\,, \tag{33}$$

corresponding to

$$\phi_d^{\mathrm{NP}}\Big|_{\mathrm{incl}} = -(10.1 \pm 4.6)^\circ\,, \qquad \phi_d^{\mathrm{NP}}\Big|_{\mathrm{excl}} = -(2.5 \pm 8.0)^\circ\,; \tag{34}$$

results of $\phi_d^{\mathrm{NP}} \approx -10^\circ$ were also recently obtained in Refs. [39, 48]. Note that the emergence of a non-zero value of ϕ_d^{NP} is caused by the large value of $|V_{ub}|$ from inclusive
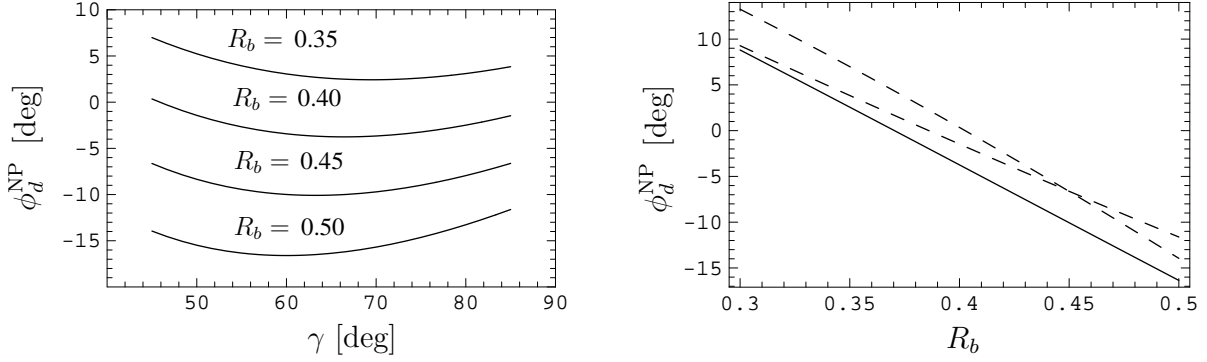
Figure 5: The determination of ϕ_d^{NP} for $\phi_d = 43.4°$. Left panel: ϕ_d^{NP} as a function of γ for various values of R_b. Right panel: ϕ_d^{NP} as a function of R_b for various values of γ (solid line: $\gamma = 65°$, dashed lines: $\gamma = (45°, 85°)$).

semileptonic decays, but that ϕ_d^{NP} is compatible with zero for $|V_{ub}|$ from exclusive decays. The consequences of the presence of a small NP phase $\phi_d^{\mathrm{NP}} \approx -10°$ are rather dramatic: from Fig. 4, one reads off the sizeable lower bound $\kappa_d \gtrsim 0.17$. Although this result hinges on the value of $|V_{ub}|_{\mathrm{incl}}$, and hence presently is not conclusive, the underlying reasoning also applies to the B_s system: even a small NP phase ϕ_s^{NP} implies considerable NP contributions to the mixing matrix element M_{12}^s.

3.4 Combined Constraints on NP through ΔM_d and ϕ_d: 2006 and 2010

We are now finally in a position to combine the constraints from both ΔM_d and ϕ_d to constrain the allowed region in the σ_d–κ_d plane. The corresponding results are shown in Fig. 6, demonstrating the power of the contours described in the previous subsections for a transparent determination of σ_d and κ_d. We see that a non-vanishing value of ϕ_d^{NP}, even as small as $\phi_d^{\mathrm{NP}} \approx -10°$, has a strong impact on the allowed space in the σ_d–κ_d plane. In both scenarios with different lattice results and different values for $|V_{ub}|$, the upper bounds of $\kappa_d \lesssim 2.5$ on the NP contributions following from the experimental value of ΔM_d are reduced to $\kappa_d \lesssim 0.5$. Values of this order of magnitude are expected, for instance, on the basis of generic field-theoretical considerations [43, 47], as well as in a recently proposed framework for "next-to-minimal flavour violation" [49, 10].

In order to determine κ_d more precisely, it is mandatory to reduce the errors of ρ_d, which come from both γ and lattice calculations. As we noted above, the value of γ can be determined – with impressive accuracy – at the LHC [41], whereas progress on the lattice side is much harder to predict, but will hopefully be made. Assuming our benchmark scenario of Tab. 2, which corresponds to the lattice results of Eq. (11), the σ_d–κ_d plane in 2010 looks like shown in Fig. 7 – and actually implies $5\,\sigma$ evidence for NP from $\phi_d^{\mathrm{NP}} = -(9.8 \pm 2.0)°$. Although there is only a small allowed region left, κ_d is still only badly constrained; for an extraction with 10% uncertainty, $f_{B_d}\hat{B}_{B_d}^{1/2}$ is required to 5% accuracy, i.e. the corresponding error in (11) has to be reduced by a factor of 2, which is the benchmark lattice theorists should strive for.
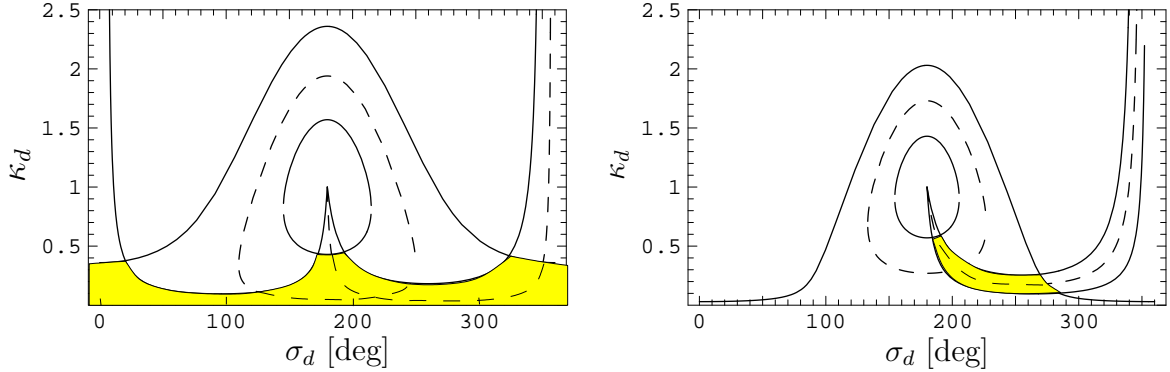
11

Figure 6: Left panel: allowed region (yellow/grey) in the σ_d–κ_d plane in a scenario with the JLQCD lattice results (10) and $\phi_d^{\mathrm{NP}}\big|_{\mathrm{excl}}$. Dashed lines: central values of ρ_d and ϕ_d^{NP}, solid lines: $\pm 1\,\sigma$. Right panel: ditto for the scenario with the (HP+JL)QCD lattice results (11) and $\phi_d^{\mathrm{NP}}\big|_{\mathrm{incl}}$.
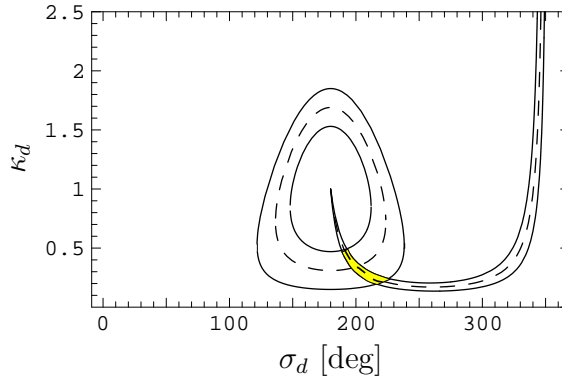

Figure 7: Allowed region in the σ_d–κ_d plane (yellow/grey) in our 2010 scenario, using the parameters collected in Tab. 2 and $\phi_d^{\mathrm{NP}} = -(9.8 \pm 2.0)°$.

4 The B_s-Meson System

4.1 Constraints on NP through ΔM_s

Let us now have a closer look at the B_s-meson system. In order to describe NP effects in a model-independent way, we parametrize them analogously to (12) and (13). The relevant CKM factor is $|V_{ts}^* V_{tb}|$. Using once again the unitarity of the CKM matrix and including next-to-leading order terms in the Wolfenstein expansion as given in Ref. [34], we have

$$\left|\frac{V_{ts}}{V_{cb}}\right| = 1 - \frac{1}{2}\left(1 - 2R_b \cos\gamma\right)\lambda^2 + \mathcal{O}(\lambda^4). \tag{35}$$

Consequently, apart from the tiny correction in λ^2, the CKM factor for ΔM_s is independent of γ and R_b, which is an important advantage in comparison with the B_d-meson system. The accuracy of the SM prediction of ΔM_s is hence limited by the hadronic mixing parameter $f_{B_s}\hat{B}_{B_s}^{1/2}$. Using the numerical values discussed in Section 2, we obtain

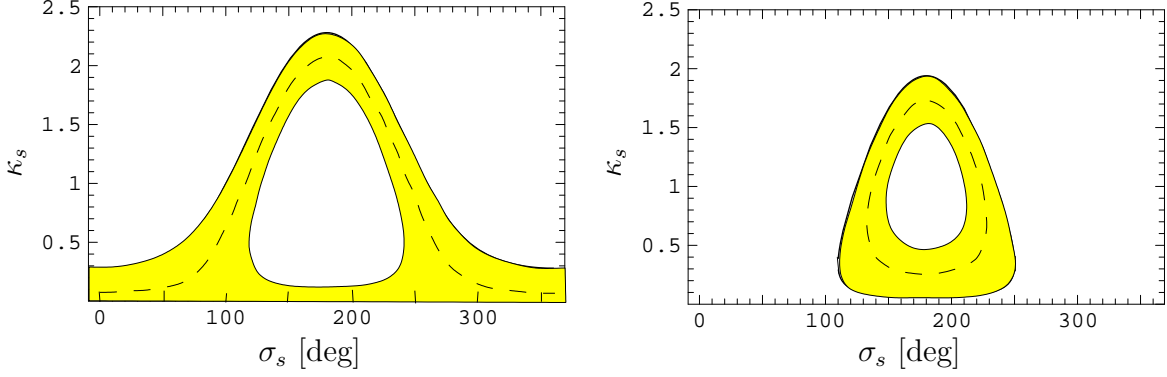$$\Delta M_s^{\mathrm{SM}}\big|_{\mathrm{JLQCD}} = (16.1 \pm 2.8)\,\mathrm{ps}^{-1},$$

12

Figure 8: The allowed regions (yellow/grey) in the σ_s–κ_s plane. Left panel: JLQCD lattice results (10). Right panel: (HP+JL)QCD lattice results (11).

$$\rho_s|_{\text{JLQCD}} = 1.08^{+0.03}_{-0.01}(\text{exp}) \pm 0.19(\text{th}),$$

$$\Delta M_s^{\text{SM}}\Big|_{(\text{HP+JL})\text{QCD}} = (23.4 \pm 3.8)\,\text{ps}^{-1},$$

$$\rho_s|_{(\text{HP+JL})\text{QCD}} = 0.74^{+0.02}_{-0.01}(\text{exp}) \pm 0.18(\text{th}), \tag{36}$$

where we made the experimental and theoretical errors explicit. The values of ρ_s, which is defined in analogy to (14), refer to the CDF measurement of ΔM_s in (4). These numbers are consistent with the SM case $\rho_s = 1$, but suffer from significant theoretical uncertainties, which are much larger than the experimental errors. Nevertheless, it is interesting to note that the (HP+JL)QCD result is $1.5\,\sigma$ below the SM; a similar pattern arises in (25), though at the $1\,\sigma$ level. Any more precise statement about the presence or absence of NP requires the reduction of theoretical uncertainties.

In Fig. 8, we show the constraints in the σ_s–κ_s plane, which can be obtained from ρ_s with the help of the B_s counterpart of (15). We see that upper bounds of $\kappa_s \lesssim 2.5$ arise from the measurement of ΔM_s. In the case of (36), the bound on σ_s following from (16) would interestingly be effective, and imply $110° \leq \sigma_s \leq 250°$. Consequently, the CDF measurement of ΔM_s leaves ample space for the NP parameters σ_s and κ_s. This situation will change significantly as soon as information about CP violation in the B_s-meson system becomes available. We shall return to this topic in Subsection 4.3.

4.2   Constraints on NP through ΔM_s and ΔM_d

It is interesting to consider the ratio of ΔM_s and ΔM_d, which can be written as follows:

$$\frac{\Delta M_s}{\Delta M_d} = \frac{\rho_s}{\rho_d} \left|\frac{V_{ts}}{V_{td}}\right|^2 \frac{M_{B_s}}{M_{B_d}} \xi^2, \tag{37}$$

where the hadronic $SU(3)$-breaking parameter ξ is defined in Subsection 2.2. In the class of NP models with "minimal flavour violation" [50],[3] which contains also the SM, we have $\rho_s/\rho_d = 1$, so that (37) allows the extraction of the CKM factor $|V_{ts}/V_{td}|$, and hence $|V_{td}|$,

---

[3]See Ref. [51] for a review, and Ref. [9] for a recent analysis addressing also the ΔM_s measurement.
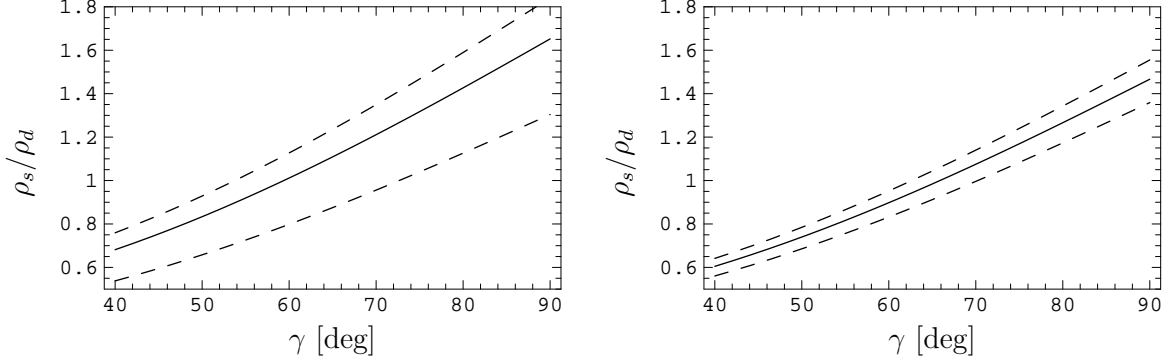
Figure 9: The dependence of ρ_s/ρ_d on γ for the central values of $\Delta M_{d,s}$ in (4). Left panel: JLQCD results (10). Right panel: (HP+JL)QCD results (11). The plots are nearly independent of R_b.

as $|V_{ts}|$ is known – to excellent accuracy – from (35). The advantage of this determination lies in the reduced theoretical uncertainty of ξ as compared to $f_{B_d}\hat{B}_{B_d}^{1/2}$.

In this paper, however, we turn the tables and constrain the ratio ρ_s/ρ_d through $\Delta M_s/\Delta M_d$. To this end, we express – in analogy to (17) – the UT side

$$R_t \equiv \frac{1}{\lambda}\left|\frac{V_{td}}{V_{cb}}\right| = \frac{1}{\lambda}\left|\frac{V_{td}}{V_{ts}}\right|\left[1 - \frac{1}{2}\left(1 - 2R_b\cos\gamma\right)\lambda^2 + \mathcal{O}(\lambda^4)\right] \tag{38}$$

in terms of R_b and γ:

$$R_t = \sqrt{1 - 2R_b\cos\gamma + R_b^2}\,, \tag{39}$$

allowing the determination of R_t through processes that are essentially unaffected by NP. The resulting value of R_t depends rather strongly on γ, which is the main source of uncertainty. Another determination of R_t that is independent of γ and R_b can, in principle, be obtained from radiative decays, in particular the ratio of branching ratios $\mathcal{B}(B \to (\rho,\omega)\gamma)/\mathcal{B}(B \to K^*\gamma)$, but is presently limited by experimental statistics; see Ref. [52] for a recent analysis.

Combining (37) and (38), we obtain the following expression for ρ_s/ρ_d:

$$\frac{\rho_s}{\rho_d} = \lambda^2\left[1 - 2R_b\cos\gamma + R_b^2\right]\left[1 + (1 - 2R_b\cos\gamma)\lambda^2 + \mathcal{O}(\lambda^4)\right]\frac{1}{\xi^2}\frac{M_{B_d}}{M_{B_s}}\frac{\Delta M_s}{\Delta M_d}\,. \tag{40}$$

In Fig. 9, we plot this ratio for the central values of ΔM_d and ΔM_s in (4), as a function of the UT angle γ for the values of ξ given in (10) and (11). We find that the corresponding curves are nearly independent of R_b and that γ is actually the key CKM parameter for the determination of ρ_s/ρ_d. The corresponding numerical values are given by:

$$\frac{\rho_s}{\rho_d}\bigg|_{\text{JLQCD}} = 1.11^{+0.02}_{-0.01}(\text{exp}) \pm 0.35(\gamma, R_b)^{+0.12}_{-0.28}(\xi)\,,$$

$$\frac{\rho_s}{\rho_d}\bigg|_{\text{(HP+JL)QCD}} = 0.99^{+0.02}_{-0.01}(\text{exp}) \pm 0.31(\gamma, R_b)^{+0.06}_{-0.08}(\xi)\,. \tag{41}$$

14

Because of the large range of allowed values of γ, Eq. (23), this ratio is currently not very stringently constrained. This situation should, however, improve significantly in the LHC era thanks to the impressive determination of γ to be obtained at the LHCb experiment. For our 2010 scenario as specified in Tab. 2, which corresponds to the right panel of Fig. 9 with $\gamma = (70 \pm 5)°$, we find:

$$\left.\frac{\rho_s}{\rho_d}\right|_{2010} = 1.07 \pm 0.09(\gamma, R_b)^{+0.06}_{-0.08}(\xi) = 1.07 \pm 0.12\,, \tag{42}$$

where we made the errors arising from the uncertainties of γ and ξ explicit, and, in the last step, added them in quadrature. Consequently, the hadronic uncertainties and those induced by γ would now be of the same size, which should provide additional motivation for the lattice community to reduce the error of ξ even further. Despite the impressive reduction of uncertainty compared to the 2006 values in (41), the numerical value in (42) would still not allow a stringent test of whether ρ_s/ρ_d equals one: to establish a $3\,\sigma$ deviation from 1, central values of $\rho_s/\rho_d = 1.4$ or 0.7 would be needed. The assumed uncertainty of γ of 5° could also turn out to be too pessimistic, in which case even more progress would be needed from the lattice side to match the experimental accuracy.

The result in (42) would not necessarily suggest that there is no physics beyond the SM. In fact, and as can be seen from Tab. 2, the central values of ρ_d and ρ_s would both be smaller than one, i.e. would both deviate from the SM picture, although the hadronic uncertainties would again not allow us to draw definite conclusions. In order to shed further light on these possible NP contributions, the exploration of CP-violating effects in the B_s-meson system is essential.

4.3   CP Violation in the B_s-System

To date, the CP-violating phase associated with B_s^0–$\bar{B}_s^0$ mixing is completely unconstrained. In the SM, it is doubly Cabibbo-suppressed, and can be written as follows:

$$\phi_s^{\mathrm{SM}} = -2\lambda^2\eta = -2\lambda^2 R_b \sin\gamma \approx -2°. \tag{43}$$

Here we used again (19) to express the Wolfenstein parameter η in terms of R_b and γ. Because of the small SM phase in (43), B_s^0–$\bar{B}_s^0$ mixing is particularly well suited to search for NP effects, which may well lead to a sizeable value of ϕ_s [53, 54]. In order to test the SM and probe CP-violating NP contributions to B_s^0–$\bar{B}_s^0$ mixing, the decay $B_s^0 \to J/\psi\phi$, which is very accessible at the LHC [18], plays a key rôle. Thanks to mixing-induced CP violation in the time-dependent angular distribution of the $J/\psi[\to \ell^+\ell^-]\phi[\to K^+K^-]$ decay products, the quantity

$$\sin\phi_s = \sin(-2\lambda^2 R_b \sin\gamma + \phi_s^{\mathrm{NP}}) \tag{44}$$

can be measured [55, 56], in analogy to the determination of $\sin\phi_d$ through $B_d^0 \to J/\psi K_{\mathrm{S}}$. After one year of data taking (which corresponds to 2 fb^{-1}), LHCb expects a measurement with the statistical accuracy $\sigma_{\mathrm{stat}}(\sin\phi_s) \approx 0.031$; adding modes such as $B_s \to J/\psi\eta, J/\psi\eta'$ and $\eta_c\phi$, $\sigma_{\mathrm{stat}}(\sin\phi_s) \approx 0.013$ is expected after five years [41]. Also ATLAS and CMS will contribute to the measurement of $\sin\phi_s$, expecting uncertainties at the 0.1 level after one year of data taking, which corresponds to 10 fb^{-1} [57, 58].
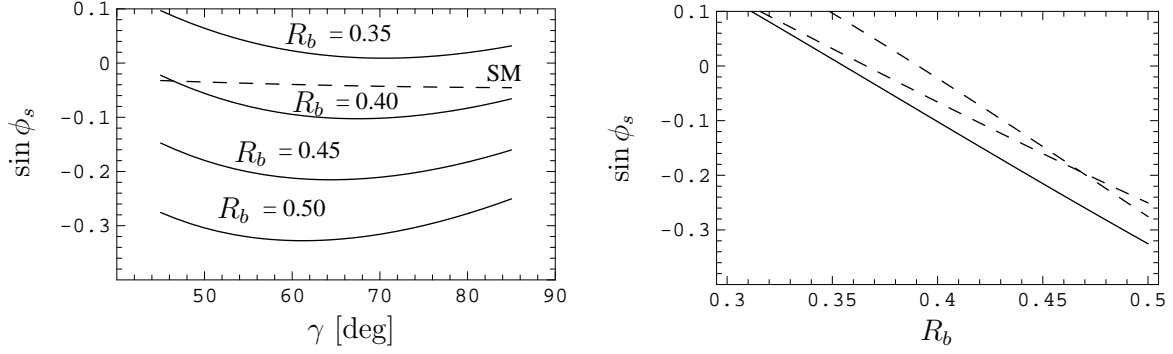
Figure 10: $\sin\phi_s$ for a scenario with flavour-universal NP, i.e. $\phi_s^{\mathrm{NP}} = \phi_d^{\mathrm{NP}}$, as specified in Eq. (45), and $\phi_d = 43.4°$. Left panel: $\sin\phi_s$ as a function of γ for various values of R_b. Right panel: $\sin\phi_s$ as a function of R_b for various values of γ (solid line: $\gamma = 65°$, dashed lines: $\gamma = (45°, 85°)$).

In order to illustrate the impact of NP effects, let us assume that the NP parameters satisfy the simple relation

$$\sigma_d = \sigma_s, \quad \kappa_d = \kappa_s, \tag{45}$$

i.e. that in particular $\phi_d^{\mathrm{NP}} = \phi_s^{\mathrm{NP}}$. This scenario would be supported by (42), although it would *not* belong to the class of models with MFV, as new sources of CP violation would be required. As we have seen in the previous section, the analysis of the B_d^0 data for $R_b^{\mathrm{incl}} = 0.45$ indicates a small NP phase around $-10°$ in the B_d-system. In the above scenario, that would imply the presence of the same phase in the B_s-system, which would interfere constructively with the small SM phase and result in CP asymmetries at the level of -20%. CP-violating effects of that size can easily be detected at the LHC. This exercise demonstrates again the great power of the B_s-meson system to reveal CP-violating NP contributions to B_q^0–$\bar{B}_q^0$ mixing. The presence of a small NP phase could actually be considerably magnified, as illustrated in Fig. 10. In specific NP scenarios, also large CP-violating phases can still arise, and are in no way excluded by the CDF measurement of ΔM_s in (4).

Let us finally also discuss the impact of CP violation measurements on the allowed region in the σ_s–κ_s plane in our 2010 scenario. To this end, we consider two cases:

  i) $(\sin\phi_s)_{\mathrm{exp}} = -0.04 \pm 0.02$, in accordance with the SM;

  ii) $(\sin\phi_s)_{\mathrm{exp}} = -0.20 \pm 0.02$, in accordance with the NP scenario of Fig. 10.

The measurement of $\sin\phi_s$ implies a twofold solution for ϕ_s and, therefore, also for ϕ_s^{NP}. However, this ambiguity can be resolved through the determination of the sign of $\cos\phi_s$, which can be fixed through the strategies proposed in Ref. [55]. In Fig. 11, we show the situation in the σ_s–κ_s plane.[4] The dotted lines refer to negative values of $\cos\phi_s$. Assuming that these are experimentally excluded, we are left with strongly restricted regions, although κ_s could still take sizeable ranges, with upper bounds $\kappa_s \approx 0.5$. In the SM-like scenario, values of σ_s around $180°$ would arise, i.e. a NP contribution with

---

[4]The closed lines agree with those shown in the right panel of Fig. 8, as our 2010 scenario is based on the (HP+JL)QCD lattice results.
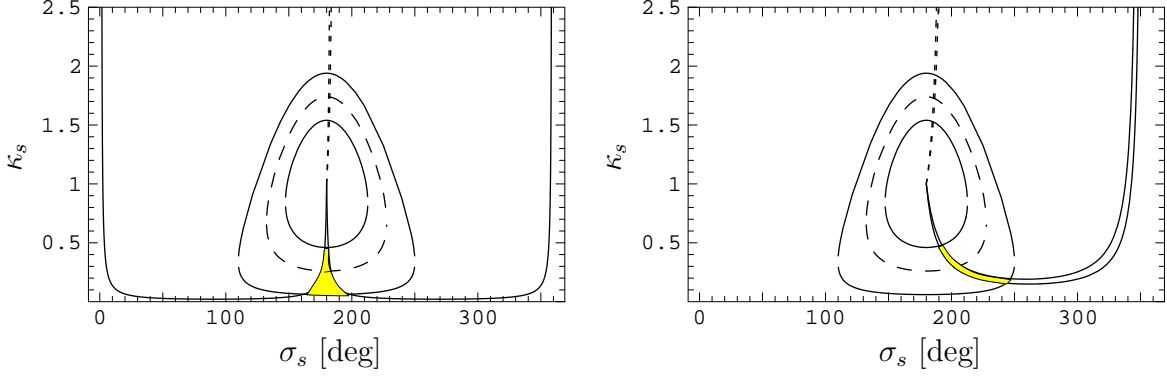
Figure 11: Combined constraints for the allowed region (yellow/grey) in the σ_s–κ_s plane through ΔM_s in (4) for the (HP+JL)QCD results (11) and CP violation measurements. Left panel: the SM scenario $(\sin\phi_s)_{\exp} = -0.04 \pm 0.02$. Right panel: a NP scenario with $(\sin\phi_s)_{\exp} = -0.20 \pm 0.02$. The solid lines correspond to $\cos\phi_s > 0$, the dotted lines to $\cos\phi_s < 0$.

a sign opposite to the SM. However, due to the absence of new CP-violating effects, the accuracy of lattice results would have to be considerably improved in order to allow the extraction of a value of κ_s incompatible with 0. On the other hand, a measurement of $(\sin\phi_s)_{\exp} = -0.20 \pm 0.02$ would give a NP signal at the $10\,\sigma$ level, with $\kappa_s \gtrsim 0.2$ from Eq. (28). In analogy to the discussion in Subsection 3.4, a determination of κ_s with 10% uncertainty requires $f_{B_s}\hat{B}_{B_s}^{1/2}$ with 5% accuracy, i.e. the corresponding error in (11) has to be reduced by a factor of 2.

Since the discussion given so far does not refer to a specific model of NP, the question arises whether there are actually extensions of the SM that still allow large CP-violating NP phases in B_s^0–$\bar{B}_s^0$ mixing.

5   Specific Models of New Physics

In this section, we address the impact of the CDF measurement of ΔM_s on two popular scenarios of NP, to wit

- an extra Z' boson with flavour non-diagonal couplings;

- generic effects in the minimal supersymmetric extension of the SM (MSSM) in the "mass insertion approximation".

We would like to stress that our examples for NP scenarios should be viewed as illustrative rather than comprehensive and are not intended to compete with more dedicated analyses.

5.1 Z' Gauge Boson with Non-Universal Couplings

Let us start with the effect of an extra $U(1)'$ gauge boson Z', which is the most simple application of the model-independent method discussed in Sections 3 and 4. The existence

of a new Z' gauge boson can induce FCNC processes at tree-level if the Z' coupling to physical fermions is non-diagonal. Such Z' bosons often occur, for instance, in the context of grand unified theories (GUTs), superstring theories, and theories with large extra dimensions, see, for instance, Refs. [59, 60]. In this paper, we illustrate the constraints on an extra Z' under the conditions that

- the Z couplings stay flavour diagonal, i.e. Z–Z' mixing is negligible and the Z does not contribute to B mixing;

- the Z' has flavour non-diagonal couplings only to left-handed quarks, which means that its effect is described by only one complex parameter.

Note that the Z' contribution to B_s mixing is related to that for hadronic, leptonic and semileptonic decays in specific models where the Z' coupling to light quarks and leptons is known; in this paper, however, we treat the Z' in a model-independent way and assume its couplings to the b_L and s_L quark fields as independent. We only discuss the B_s-system and closely follow the notations of Ref. [61], where an earlier analysis of this scenario was given.

A purely left-handed off-diagonal Z' coupling to b and s quarks gives the following contribution to M_{12}^s:[5]

$$M_{12}^{s,Z'} = \frac{G_{\mathrm{F}}}{\sqrt{2}} \rho_L^2 e^{2i\phi_L} \frac{4}{3} \hat{\eta}^B \hat{B}_{B_s} f_{B_s}^2 M_{B_s} , \qquad (46)$$

where $\rho_L e^{i\phi_L} \equiv (g' M_Z)/(g M_{Z'}) B_{sb}^L$ is defined in terms of the SM $U_Y(1)$ gauge coupling g, the $U(1)'$ coupling g', the respective gauge boson masses $M_{Z,Z'}$ and the FCNC coupling B_{sb}^L of the Z' to b_L and s_L. Generically, one would expect $g/g' = \mathcal{O}(1)$, if both $U(1)$ groups have the same origin, for instance in a GUT framework, and $M_Z/M_{Z'} = \mathcal{O}(0.1)$ for a TeV-scale Z'. If in addition the size of the Z' couplings B^L is set by the quarks' Yukawa couplings, one also expects $|B_{sb}^L| \approx |V_{ts}^* V_{tb}|$ and $\rho_L = \mathcal{O}(10^{-3})$.

The impact of the CDF measurement of ΔM_s on this model can be directly read off Fig. 8 through the identifications

$$\rho_L \leftrightarrow (\kappa_s/f)^{1/2}, \qquad \phi_L \leftrightarrow \sigma_s/2 ,$$

with

$$f = \frac{16\pi^2}{\sqrt{2}} \frac{1}{G_{\mathrm{F}} M_W^2 S_0(x_t) |V_{ts}|^2} = (3.57 \pm 0.01) \cdot 10^5 .$$

Presently, values of κ_s as large as 2.5 are still allowed, see Fig. 8, which corresponds to

$$\rho_L < 2.6 \cdot 10^{-3} . \qquad (47)$$

If a non-zero value of the NP phase ϕ_s^{NP} should be measured at the LHC, this value can be immediately translated into a lower bound on ρ_L, using (28). Assuming $\phi_s^{\mathrm{NP}} = -10°$, one has

$$\sin\phi_s = -0.2 \leftrightarrow \rho_L > 0.5 \cdot 10^{-3} , \qquad (48)$$

---

[5]Strictly speaking, $\hat{\eta}^B \hat{B}_{B_s}$ should be taken at LO accuracy; here, we effectively absorb the (small) difference between LO and NLO expressions into the definition of ρ_L.

and $\kappa_s < 0.5 \leftrightarrow \rho_L < 1.2 \cdot 10^{-3}$. Any more precise constraint on ρ_L will depend on the progress in lattice determinations of $f_{B_s} \hat{B}_{B_s}^{1/2}$.

The upper bound on ρ_L given in Eq. (47) can be converted into a lower bound on the Z' mass:

$$1.5 \, \text{TeV} \left(\frac{g'}{g} \right) \left| \frac{B_{sb}^L}{V_{ts}} \right| < M_{Z'} \, . \tag{49}$$

In the scenario of (48), there is also an upper bound and the lower bound is raised:

$$3 \, \text{TeV} \left(\frac{g'}{g} \right) \left| \frac{B_{sb}^L}{V_{ts}} \right| < M_{Z'} < 7.5 \, \text{TeV} \left(\frac{g'}{g} \right) \left| \frac{B_{sb}^L}{V_{ts}} \right| \, . \tag{50}$$

We would like to stress again that these bounds apply to a model where the Z' has flavour non-diagonal couplings only to left-handed quarks. Eq. (50) can be compared to the existing lower bounds on the Z' mass from direct searches, as for instance quoted by CDF [62]; these limits are model-dependent, but in the ballpark of $\sim 800 \, \text{GeV}$, which is perfectly compatible with (50). On the other hand, if a Z' was found in direct searches at the Tevatron or the LHC, the bounds on ρ_L would constrain its couplings. This is particularly interesting in a framework with nearly family-universal couplings and illustrates the potential synergy between direct searches for NP and constraints from flavour physics.

Note that (47) can also be translated into an upper bound on the branching ratio of $B_s \to \mu^+ \mu^-$, at least if the coupling of the Z' to $\mu^+ \mu^-$ is known. The relevance of such a bound is not quite clear, however, since we have set the coupling of the Z' to right-handed fermions to 0.

5.2 MSSM in the Mass Insertion Approximation

Let us now discuss B mixing in supersymmetry. Whereas in the SM flavour violation is parametrized by the CKM matrix, in SUSY there are many more possible ways in which both lepton and quark flavours can change. This is because scalar quarks and leptons carry the flavour quantum numbers of their SUSY partners, which implies that flavour violation in the scalar sector can lead to flavour violation in the observed fermionic sector of the theory. The parameters controlling flavour violation in the MSSM are quite numerous – there are about 100 soft SUSY breaking parameters which could give rise to huge – and unobserved – flavour violation. One way to defuse this so-called SUSY flavour problem is to assume that the squark (and slepton) masses are approximately aligned with the quark (and lepton) masses. "Alignment" means that, in the basis of physical states, where the fermion masses are diagonal, the scalar mass matrices are approximately diagonal as well. In this case, one can treat the off-diagonal terms in the sfermion mass matrices,

$$(\delta_{ij}^f)_{AB} \equiv (\Delta m_{ij}^2)_{AB} / m_{\tilde{f}}^2 \, ,$$

as perturbations. Here $i, j = 1, 2, 3$ are family indices, $A, B = L, R$ refers to the "chirality"[6] of the sfermions and $m_{\tilde{f}}$ is the average sfermion mass. This so-called mass insertion approximation (MIA) has been first introduced in Ref. [63], and was extensively applied

---

[6]Sfermions are scalar particles and hence have no chirality; the labels L and R refer to the fact that they are the SUSY partners of left- and right-handed quark fields, respectively.

to FCNC and CP-violating phenomena in Ref. [64]. Its strength is the fact that it is independent of specific model assumptions on the values of soft SUSY-breaking parameters, but its weakness is that there are many free parameters, so there is a certain loss of predictive power. In this paper, we do not attempt a sophisticated analysis, which will only be possible once a full NLO calculation of the corresponding short-distance functions has become available, which is in preparation, see Ref. [65]. Rather, we would like to illustrate the impact of the constraints from ΔM_s on the dominant mass insertions, along the lines of, for instance, Refs. [66, 8]. Bounds on mass insertions from B_d mixing have been investigated in Ref. [67].

In supersymmetric theories the effective Hamiltonian $\mathcal{H}_{\text{eff}}^{\Delta B=2}$ responsible for B mixing, see Eq. (1), is generated by the SM box diagrams with W exchange and box diagrams mediated by charged Higgs, neutralino, photino, gluino and chargino exchange. For small values of $\tan\beta_{\text{SUSY}}$, which is the ratio of vacuum expectation values of the two MSSM Higgs doublets, the Higgs contributions are suppressed by the quark masses and can be neglected. Photino and neutralino diagrams are also heavily suppressed compared to those from gluino and chargino exchange, due to the smallness of the electroweak couplings compared to α_s. The gluino contribution was calculated in Ref. [64], the chargino one in Ref. [68]. The analysis of Ref. [66] has shown that the chargino contributions are also very small, so that the B_s^0–$\bar{B}_s^0$ transition matrix element is given, to good accuracy, by

$$M_{12}^s = M_{12}^{s,\text{SM}} + M_{12}^{s,\tilde{g}} \,, \tag{51}$$

where $M_{12}^{s,\text{SM}}$ and $M_{12}^{s,\tilde{g}}$ indicate the SM and gluino contributions, respectively. It turns out that the largest contribution to $M_{12}^{s,\tilde{g}}$ comes from terms in $(\delta_{23}^d)_{LL}(\delta_{23}^d)_{RR}$, whereas chirality flipping LR and RL mass insertions are only poorly constrained from B_s mixing, but dominantly enter $b \to s\gamma$ decays. The bounds on $(\delta_{23}^d)_{LR}$ and $(\delta_{23}^d)_{RL}$ posed by the corresponding branching ratio have been investigated in Ref. [69], a recent update can be found in Ref. [70]. As for the chirality-conserving mass insertions, the impact of the D0 bound (5) has been studied in Refs. [6, 8]. Here we set all but one mass insertion to 0 and restrict ourselves to bounds on $(\delta_{23}^d)_{LL}$ and the impact of a future measurement of ϕ_s on these bounds.

The effective $\Delta B = 2$ Hamiltonian in the MSSM contains a total of eight operators as compared to only one in the SM. The corresponding hadronic matrix elements (bag parameters) have been calculated, in quenched approximation, in Ref. [71]. The evolution of the Wilson coefficients from M_{S}, the scale where the SUSY particles are integrated out, to m_b is known to next-to-leading order [72, 67]. The expression for ΔM_s in the MSSM then depends on M_{S}, $m_{\tilde{q}}$, the average sfermion mass, and $m_{\tilde{g}}$, the gluonino mass. We take $m_{\tilde{q}} = 500\,\text{GeV} = m_{\tilde{g}}$ and also $M_{\text{S}} = 500\,\text{GeV}$ as illustrative values. We then obtain the constraints on $\text{Re}\,(\delta_{23}^d)_{LL}$ and $\text{Im}\,(\delta_{23}^d)_{LL}$ shown in Fig. 12. The closed curves in the centre of the plots correspond to the allowed values of the real and imaginary part of $(\delta_{23}^d)_{LL}$ after the measurement of ΔM_s; note that the experimental value of ΔM_s is incompatible with the SM prediction at $1.5\,\sigma$ level when the (HP+JL)QCD lattice data are used, Eq. (36), hence the origin is excluded in the right panel. The open lines correspond to constraints imposed by a measurement of the mixing phase ϕ_s, as explained in the caption. It is obvious that at present no value of ϕ_s is excluded and that the precise measurement of the mixing phase, expected to take place at the LHC, will considerably restrict the parameter space of SUSY mass insertions.
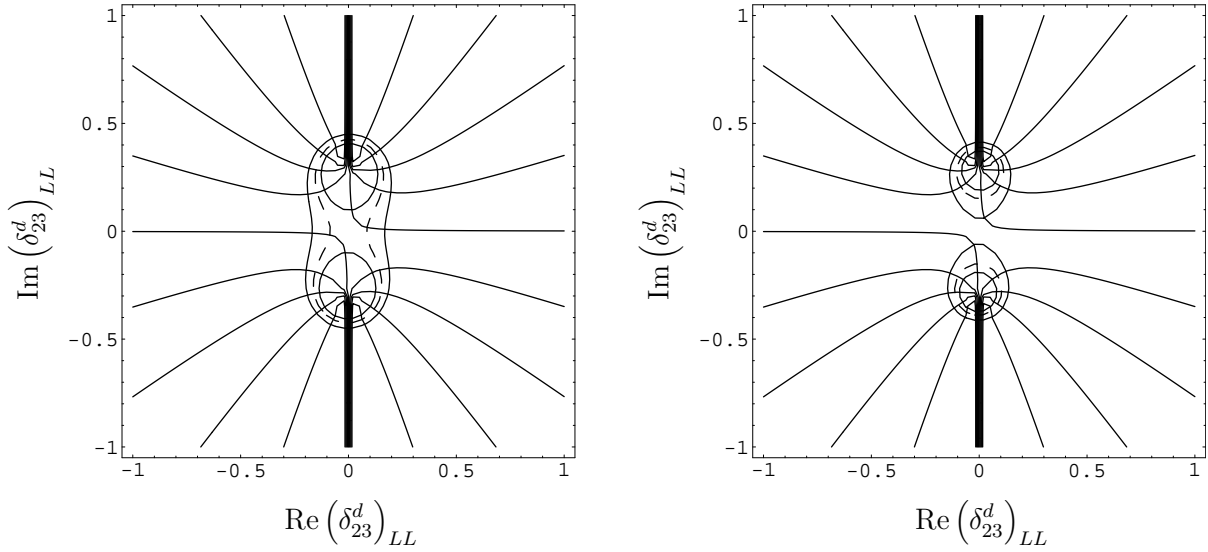
20

Figure 12: $1\,\sigma$ constraints on $(\delta_{23}^d)_{LL}$ from ΔM_s (closed lines). Left panel: JLQCD results (10), right panel: (HP+JL)QCD results (11). The open lines denote constraints posed by a measurement of ϕ_s: the curves in the upper right and lower left quadrant correspond, from bottom to top in the upper quadrant, and top to bottom in the lower quadrant, to $\phi_s \in \{0°, 36°, 72°, 108°, 144°\}$, whereas those in the upper left and lower right quadrant correspond to phases between $-180°$ and $0°$.

If SUSY is found at the LHC, and the gluino and average squark masses are measured, the results from MIA analyses of flavour processes will help to constrain the soft SUSY breaking terms and hence the – yet to be understood – mechanism of SUSY breaking. Given the sheer number of these terms (about 100), it will be very difficult to resolve the richness of SUSY breaking from direct SUSY searches alone, which will have to be complemented by constraints (or measurements) from flavour physics – which, in turn, will become more expressive, once the direct searches will have provided the relevant mass scales.

6   Conclusions and Outlook

The FCNC processes of B_d^0–$\bar{B}_d^0$ and B_s^0–$\bar{B}_s^0$ mixing offer interesting probes to search for signals of physics beyond the SM. Although the former phenomenon is well established since many years, the latter has only just been observed at the Tevatron, thereby raising in particular the question of the implications for the parameter space of NP.

The current situation can be summarized as follows: the experimental value of the mass difference ΔM_d and the recently measured ΔM_s agree with the SM. However, the SM predictions of these quantities suffer from large uncertainties. In particular, some lattice calculations ((HP+JL)QCD) indicate a value of ΔM_s^{SM} that is $1.5\,\sigma$ larger than the experimental CDF value, whereas the JLQCD results show no such effect. A similar pattern arises at the $1\,\sigma$ level in the B_d-meson system. In view of these uncertainties, values

of $\kappa_{d,s}$, the strength of the NP contributions to $B_{d,s}$ mixing, as large as 2.5 are still allowed by the experimental values of $\Delta M_{d,s}$, and the new CP-violating phases $\sigma_{d,s}$ are essentially unconstrained. Complementary information is provided by CP violation. Interestingly, the impressive measurement of mixing-induced CP violation in $B_d^0 \to J/\psi K_S$ (and similar modes) at the B factories may indicate a small – but noticeable – CP-violating NP phase ϕ_d^{NP} around $-10°$, which would have a drastic impact on the allowed region in the σ_d–κ_d plane and would result in a lower bound on κ_d of ≈ 0.2. In any case, the experimentally excluded large values of ϕ_d^{NP} reduce the upper bound $\kappa_d \approx 2.5$ significantly to 0.5. On the other hand, no information about ϕ_s^{NP} is currently available, so that we are left with the large range of $0 \lesssim \kappa_s \lesssim 2.5$.

The following quantities play a key rôle for these studies: mixing:

- The CKM parameters γ and $R_b \propto |V_{ub}/V_{cb}|$, which enter the analysis of B_d^0–$\bar{B}_d^0$ mixing in a complementary manner. Whereas the UT angle γ is currently a significant source of uncertainty for the SM prediction of ΔM_d (and $\Delta M_s/\Delta M_d$), R_b is crucial for the detection of a NP phase ϕ_d^{NP}. Thanks to the LHCb experiment, the situation for γ will improve dramatically in the future, where we assumed $\gamma = (70 \pm 5)°$ in our 2010 benchmark scenario. Concerning R_b, the error of $|V_{cb}|$ has already a marginal impact. However, there is currently a 1σ discrepancy between the inclusive and exclusive determinations of $|V_{ub}|$, pointing towards $\phi_d^{\mathrm{NP}} \approx -10°$ and $\phi_d^{\mathrm{NP}} \approx 0°$, respectively. Consequently, it is crucial to clarify this situation and to reduce the uncertainty of $|V_{ub}|$. In our benchmark scenario, we assume that the central value of $|V_{ub}|_{\mathrm{incl}}$ will be confirmed, and that its uncertainty shrinks to 5% due to experimental and theoretical progress. It is an advantage of the B_s-meson system that the SM analysis of its mixing parameters is essentially unaffected by CKM uncertainties.

- The hadronic parameters $f_{B_q} \hat{B}_{B_q}^{1/2}$, which enter the SM predictions of ΔM_q. For a determination of κ_q with 10% uncertainty, the errors of the (HP+JL)QCD lattice results have to be reduced by a factor of 2. The hadronic uncertainties are smaller if one considers the ratio $\Delta M_s/\Delta M_d$, involving the $SU(3)$-breaking parameter ξ. Presently, there is no indication of this ratio to deviate from its SM prediction, but there is still a large uncertainty. In our 2010 benchmark scenario, the error from ξ would match that from γ. Nevertheless, it will probably be challenging to detect NP through deviations of ρ_s/ρ_d from 1. Moreover, a result in agreement with 1 does not allow any conclusion about the presence or absence of NP, as ρ_s and ρ_d may both deviate similarly from 1, except for excluding certain NP scenarios, like for instance Higgs penguins enhanced by large values of $\tan\beta_{\mathrm{SUSY}}$.

Concerning the prospects for the search for NP through B_s^0–$\bar{B}_s^0$ mixing at the LHC, it will be very challenging if essentially no CP-violating effects will be found in $B_s^0 \to J/\psi\phi$ (and similar decays). On the other hand, as we demonstrated in our analysis, even a small phase $\phi_s^{\mathrm{NP}} \approx -10°$ (inspired by the B_d data) would lead to CP asymmetries at the -20% level, which could be unambiguously detected after a couple of years of data taking, and would not be affected by hadronic uncertainties. Conversely, the measurement of such an asymmetry would allow one to establish lower bounds on the strength of NP contribution – even if hadronic uncertainties still preclude a direct extraction of this contribution from ΔM_s – and to dramatically reduce the allowed region in the NP parameter space. In fact,

the situation may be even more promising, as specific scenarios of NP still allow large new phases in B_s^0–$\bar{B}_s^0$ mixing, also after the measurement of ΔM_s. We have illustrated this exciting feature by considering models with an extra Z' boson and SUSY scenarios with an approximate alignment of quark and squark masses.

In essence, the lesson to be learnt from the CDF measurement of ΔM_s is that NP may actually be hiding in B_s^0–$\bar{B}_s^0$ mixing, but is still obscured by parameter uncertainties, some of which will be reduced by improved statistics at the LHC, whereas others require dedicated work of, in particular, lattice theorists. The smoking gun for the presence of NP in B_s^0–$\bar{B}_s^0$ mixing will be the detection of a non-vanishing value of ϕ_s^{NP} through CP violation in $B_s^0 \to J/\psi\phi$. Let us finally emphasize that the current B-factory data may show – in addition to $\phi_d^{\mathrm{NP}} \approx -10°$ – other first indications of new sources of CP violation through measurements of $B_d^0 \to \phi K_{\mathrm{S}}$ and $B \to \pi K$ decays, which may point towards a modified electroweak penguin sector. All these examples are yet another demonstration that flavour physics is not an optional extra, but an indispensable ingredient in the pursuit of NP, also and in particular in the era of the LHC.

Acknowledgements

References

[1] E. Barberio *et al.* [HFAG], hep-ex/0603003; updated results available at `http://www.slac.stanford.edu/xorg/hfag/`.

[2] *B* Oscillations Working Group: `http://lepbosc.web.cern.ch/LEPBOSC/`.

[3] G. Gomez-Ceballos [CDF coll.], talk at FPCP 2006, `http://fpcp2006.triumf.ca`.

[4] V. Abazov *et al.* [D0 coll.], hep-ex/0603029.

[5] M. Carena *et al.*, hep-ph/0603106.

[6] M. Ciuchini and L. Silvestrini, hep-ph/0603114.

[7] L. Velasco-Sevilla, hep-ph/0603115.

[8] M. Endo and S. Mishima, hep-ph/0603251.

[9] M. Blanke, A.J. Buras, D. Guadagnoli and C. Tarantino, hep-ph/0604057.

[10] Z. Ligeti, M. Papucci and G. Perez, hep-ph/0604112.

[11] J. Foster, K.I. Okumura and L. Roszkowski, hep-ph/0604121.

[12] G. Buchalla, A.J. Buras and M.E. Lautenbacher, *Rev. Mod. Phys.* **68** (1996) 1125.

[13] N. Cabibbo, *Phys. Rev. Lett.* **10** (1963) 531.

[14] M. Kobayashi and T. Maskawa, *Prog. Theor. Phys.* **49** (1973) 652.

[15] Tevatron Electroweak Working Group, hep-ex/0507091.

[16] T. Inami and C.S. Lim, *Prog. Theor. Phys.* **65** (1981) 297 [E: **65** (1981) 1772].

[17] S.L. Glashow, J. Iliopoulos and L. Maiani, *Phys. Rev.* **D2** (1970) 1285.

[18] P. Ball *et al.*, hep-ph/0003238.

[19] L. Wolfenstein, *Phys. Rev. Lett.* **51** (1983) 1945.

[20] S. Eidelman *et al.* [Particle Data Group], *Phys. Lett.* **B592** (2004) 1.

[21] R. Fleischer, *Phys. Rept.* **370** (2002) 537.

[22] O. Buchmüller and H. Flächer, hep-ph/0507253.

[23] P. Gambino and N. Uraltsev, *Eur. Phys. J.* **C34** (2004) 181.

[24] M. Okamoto *et al.*, *Nucl. Phys. Proc. Suppl.* **140** (2005) 461;
E. Gulez *et al.*, *Phys. Rev.* **D73** (2006) 074502.

[25] A. Khodjamirian *et al.*, *Phys. Rev.* **D62** (2000) 114002;
P. Ball and R. Zwicky, *JHEP* **0110** (2001) 019; *Phys. Rev.* **D71** (2005) 014015; *Phys. Rev.* **D71** (2005) 014029; *Phys. Lett.* **B625** (2005) 225.

[26] J.R. Andersen and E. Gardi, *JHEP* **0601** (2006) 097.

[27] H. Leutwyler, *Phys. Lett.* **B378** (1996) 313.

[28] A.S. Kronfeld and S.M. Ryan, *Phys. Lett.* **B543** (2002) 59.

[29] S. Aoki *et al.* [JLQCD coll.], *Phys. Rev. Lett.* **91** (2003) 212001.

[30] A. Gray *et al.* [HPQCD coll.], *Phys. Rev. Lett.* **95** (2005) 212001.

[31] M. Okamoto, *PoS* **LAT2005** (2005) 013.

[32] F. Palombi, M. Papinutto, C. Pena and H. Wittig [ALPHA coll.], *PoS* **LAT2005** (2005) 214.

[33] M. Creutz, hep-lat/0603020;
C. Bernard, M. Golterman, Y. Shamir and S. Sharpe, hep-lat/0603027;
C. Bernard, M. Golterman and Y. Shamir, hep-lat/0604017.

[34] A.J. Buras, M.E. Lautenbacher and G. Ostermaier, *Phys. Rev.* **D50** (1994) 3433.

[35] E. Blucher *et al.*, hep-ph/0512039.

[36] G. Cavoto *et al.*, hep-ph/0603019.

[37] J. Charles *et al.* [CKMfitter Group], *Eur. Phys. J.* **C41** (2005) 1; for the most recent updates, see `http://ckmfitter.in2p3.fr/`.

[38] M. Bona *et al.* [UTfit Collaboration], *JHEP* **0507** (2005) 028; for the most recent updates, see `http://utfit.roma1.infn.it/`.

[39] A.J. Buras, R. Fleischer, S. Recksiegel and F. Schwab, *Eur. Phys. J.* **C45** (2006) 701.

[40] C.W. Bauer, I.Z. Rothstein and I.W. Stewart, *Phys. Rev. Lett.* **94** (2005) 231802; hep-ph/0510241.

[41] O. Schneider, talk at the "Flavour in the era of the LHC" workshop, CERN, November 2005, `http://cern.ch/flavlhc`.

[42] A.B. Carter and A.I. Sanda, *Phys. Rev. Lett.* **45** (1980) 952; *Phys. Rev.* **D23** (1981) 1567;
I.I. Bigi and A.I. Sanda, *Nucl. Phys.* **B193** (1981) 85.

[43] R. Fleischer and T. Mannel, *Phys. Lett.* **B506** (2001) 311.

[44] R. Fleischer, *J. Phys.* **G32** (2006) R71.

[45] R. Fleischer, *Phys. Lett.* **B562** (2003) 234; *Nucl. Phys.* **B659** (2003) 321.

[46] R. Fleischer and J. Matias, *Phys. Rev.* **D66** (2002) 054009.

[47] R. Fleischer, G. Isidori and J. Matias, *JHEP* **0305** (2003) 053.

[48] M. Bona *et al.* [UTfit Collaboration], *JHEP* **0603** (2006) 080.

[49] K. Agashe, M. Papucci, G. Perez and D. Pirjol, hep-ph/0509117.

[50] G. D'Ambrosio, G.F. Giudice, G. Isidori and A. Strumia, *Nucl. Phys.* **B645** (2002) 155;
A.J. Buras *et al.*, *Phys. Lett.* **B500** (2001) 161.

[51] A.J. Buras, *Acta Phys. Polon.* **B34** (2003) 5615.

[52] P. Ball and R. Zwicky, *JHEP* **0604** (2006) 046.

[53] Y. Nir and D.J. Silverman, *Nucl. Phys.* **B345** (1990) 301.

[54] G.C. Branco, T. Morozumi, P.A. Parada and M.N. Rebelo, *Phys. Rev.* **D48** (1993) 1167.

[55] I. Dunietz, R. Fleischer and U. Nierste, *Phys. Rev.* **D63** (2001) 114015.

[56] A.S. Dighe, I. Dunietz and R. Fleischer, *Eur. Phys. J.* **C6** (1999) 647.

[57] M. Smizanska (ATLAS collaboration), private communication.

[58] T. Speer (CMS collaboration), private communication.

[59] P. Langacker and M. Plümacher, *Phys. Rev.* **D62** (2000) 013006.

[60] M. Cvetic, G. Shiu and A.M. Uranga, *Phys. Rev. Lett.* **87** (2001) 201801; *Nucl. Phys.* **B615** (2001) 3;
M. Cvetic, P. Langacker and G. Shiu, *Phys. Rev.* **D66** (2002) 066004.

[61] V. Barger, C.W. Chiang, J. Jiang and P. Langacker, *Phys. Lett.* **B596** (2004) 229.

[62] A. Abulencia *et al.* [CDF coll.], hep-ex/0602045; hep-ex/0603006.

[63] L.J. Hall, V.A. Kostelecky and S. Raby, *Nucl. Phys.* **B267** (1986) 415.

[64] F. Gabbiani *et al.*, *Nucl. Phys.* **B477** (1996) 321.

[65] M. Ciuchini *et al.*, *PoS* **HEP2005** (2006) 221.

[66] P. Ball, S. Khalil and E. Kou, *Phys. Rev.* **D69** (2004) 115011.

[67] D. Becirevic *et al.*, *Nucl. Phys.* **B634** (2002) 105.

[68] E. Gabrielli and S. Khalil, *Phys. Rev.* **D67** (2003) 015008.

[69] M. Ciuchini, E. Franco, A. Masiero and L. Silvestrini, *Phys. Rev.* **D67** (2003) 075016 [E: **D68** (2003) 079901].

[70] L. Silvestrini, hep-ph/0510077.

[71] D. Becirevic *et al.*, *JHEP* **0204** (2002) 025.

[72] A.J. Buras, S. Jäger and J. Urban, *Nucl. Phys.* **B605** (2001) 600.